Proteomic analysis of anti-angiogenic effects by conbercept in the mice with oxygen induced retinopathy

Ji Jin[1,2], Lei Chen[3], Gao–Qin Liu[1], Pei–Rong Lu[1]

[1]Department of Ophthalmology, the First Affiliated Hospital of Soochow University, Suzhou 215006, Jiangsu Province, China
[2]Department of Ophthalmology, the Second Affiliated Hospital of Soochow University, Suzhou 215004, Jiangsu Province, China
[3]Department of Ophthalmology, Children's Hospital of Soochow University, Suzhou 215025, Jiangsu Province, China
Correspondence to: Pei-Rong Lu. Department of Ophthalmology, the First Affiliated Hospital of Soochow University, No.188 Shizi Street, Suzhou 215006, Jiangsu Province, China. lupeirong@suda.edu.cn

Abstract

● **AIM:** To analyze the retinal proteomes with and without conbercept treatments in mice with oxygen-induced retinopathy (OIR) and identify proteins involved in the molecular mechanisms mediated by conbercept.

● **METHODS:** OIR was induced in fifty-six C57BL/6J mouse pups and randomly divided into four groups. Group 1: Normal17 (*n*=7), mice without OIR and treated with normal air. Group 2: OIR12/EXP1 (*n*=14), mice received 75% oxygen from postnatal day (P) 7 to 12. Group 3: OIR17/Control (*n*=14), mice received 75% oxygen from P7 to P12 and then normal air to P17. Group 4: Lang17/EXP2 (*n*=21), mice received 75% oxygen from P7 to P12 with intravitreal injection of 1 μL conbercept at the concentration of 10 mg/mL at P12, and then normal air from P12 to P17. Liquid Chromatography-Mass Spectrometry (LC-MS)/MS data were reviewed to find proteins that were up-regulated after the conbercept treatment. Gene ontology (GO) analysis was performed of conbercept-mediated changes in proteins involved in single-organism processes, biological regulation, cellular processes, immune responses, metabolic processes, locomotion and multiple-organism processes.

● **RESULTS:** Conbercept induced a reversal of hypoxia-inducible factor 1 signaling pathway as revealed by the Kyoto Encyclopedia of Genes and Genomes (KEGG) analysis and also induced down-regulation of proteins involved in blood coagulation and fibrin clot formation as demonstrated by the Database for Annotation, Visualization and Integrated Discovery (DAVID) and the stimulation of interferon genes studies. These appear to be risk factors of retinal fibrosis. Additional conbercept-specific fibrosis risk factors were also identified and may serve as therapeutic targets for fibrosis.

● **CONCLUSION:** Our studies reveal that many novel proteins are differentially regulated by conbercept. The new insights may warrant a valuable resource for conbercept treatment.

● **KEYWORDS:** anti-vascular endothelial growth factor; conbercept; retinopathy; fibrosis; proteomic analysis

INTRODUCTION

Pathological retinal neovascularization, an abnormal blood vessel growth in the retina, occurs where there is retinal ischemia. It is one of the most common causes of vision loss[1]. Some studies have revealed that many angiogenic factors are involved during the development of retinal neovascularization[2-4], of which vascular endothelial growth factor (VEGF) is mostly thought to be the key mediator of neovascularization[5]. Michaelson[6] firstly suggested the presence of an angiogenic factor responsible for neovascularization in retinopathy. VEGF plays an vital role in the regulation of angiogenesis by stimulating proliferation and vascular endothelial cell migration[7], enhances vascular permeability, and drives the formation of choroidal neovascularization[8-9]. Patients with increased levels of VEGF in ocular fluids and active neovascular ocular disease were also reported[5]. The rental injury may also disturb homeostatic balance, showing in elevated cell proliferation, cellular shape change, VEGF production, and promote retinal fibrosis which ultimately leads to blindness[10].

Using the anti-VEGF agents for treating ocular disorders has been introduced for over 10y[11]. It is known that anti-VEGF drug is effective in many diseases, such as diabetic retinopathy[12] and neovascular age-related macular degeneration (AMD)[9,13]. Blocking VEGF functions using

local intravitreal injections of VEGF receptor antibodies, VEGF neutralizing antibodies, or VEGF receptor chimeric proteins has been reported with clinical success in eye neovascularization[14]. Anti-VEGF antibodies, such as ranibizumab or bevacizumab, are mainly used as the first-line treatment for neovascular AMD[15]. They have been developed to antagonize the function of VEGF, decreasing the plasma leakage through incompetent neovasculature and result in a temporary improvement in vision[16]. However, in some diseases such as retinal branch vein occlusion, diabetic retinopathy, repeated administration over time may cause a reduction in bio-efficiency. The repeated intravitreal injection of anti-VEGF drugs in the treatment of ocular disorders may induce intraocular pressure fluctuations and long-term suppression of neurotrophic cytokines[17]. Some patients have experienced a gradual efficacy loss of these anti-VEGF drugs after repeated administration over time with the reported tolerance rate at 2%-10%[18-19].

Conbercept (KH902) is among the most recent anti-VEGF drugs approved for treating neovascular AMD by the China Food and Drug Administration in December 2013. It appears to have higher binding affinity, longer clearance time, and lower VEGF dissociation rate than other anti-VEGF drugs[20]. Conbercept acts as a soluble receptor decoy that blocks all isoforms of VEGF-A, VEGF-B, VEGF-C, and placental growth factor (PlGF) and also has a long half-life in vitreous[20]. Preclinical studies have demonstrated that conbercept has anti-angiogenesis activity not only in ocular neovascular disease models but also in tumor models[9]. Zhang et al[17] had reported that repeated intravitreal injections of conbercept were well tolerated in AMD patients; however, more studies were required to confirm its long-term efficacy and safety.

Proteome analyses of various retina diseases, such as AMD, diabetic retinopathy and retinal degeneration using rat[21] or human[22] samples have been reported. Besides, a proteomics study on the rabbit retinal receiving high frequency intravitreal injection of conbercept had also suggested that there was no significant difference in inflammation or apoptosis associated proteins[23]. The retinal proteome analysis in mouse model of oxygen-induced retinopathy (OIR) has been conducted[24-25]; however, the effect of conbercept on retinal proteomic changes in OIR mice has not yet been reported. In addition, previous studies have suggested that anti-VEGF treatment may result in the up-regulation of hypoxia-inducible factors-1 (HIF-1) protein[26]. The effect of conbercept on the regulation of HIF-1 protein in OIR model had also been studied.

In this study, we aimed to explore the effects of conbercept on the molecular mechanism in retinal neovascularization using mice with OIR. Additionally, we assessed the conbercept-induced changes in retinal protein expression to identify the underlying molecular mechanisms of conbercept in OIR.

MATERIALS AND METHODS

Ethical Approval All animal experiments were performed under the Guidelines for the Care and Use of Laboratory Animals of the Chinese Medical Academy and were performed in accordance with the Association for Research in Vision and Ophthalmology (ARVO) Statement for the Use of Animals in Ophthalmic and Vision Research, Soochow University, Suzhou, China, and were approved by the Animal Care Committee (Suzhou, China).

Establishment of a Mouse Model with OIR C57B6 mice were obtained from Shanghai SLAC Laboratory Animal Co. Ltd. (Shanghai, China) and fed with a standard laboratory diet and water in a specific pathogen-free condition with a 12-hour light-dark cycle.

OIR was induced in fifty-six C57BL/6J mouse pups as previously described[27]. Mice were randomly divided into four groups. The experimental protocol was presented in Figure 1A. Group 1: Normal17 (n=7), mice without OIR and treated with normal air. Group 2: OIR12/EXP1 (n=14), mice received 75% oxygen from postnatal day (P) 7 to 12. Group 3: OIR17/Control (n=14), mice received 75% oxygen from P7 to P12 and then normal air to P17. Group 4: Lang17/EXP2 (n=21), mice received 75% oxygen from P7 to P12 with intravitreal injection of 1 μL conbercept at the concentration of 10 mg/mL at P12, and then normal air from P12 to P17.

Intravitreal Injection We performed intravitreal injection based on the protocol proposed by Chiu et al[28] with slight modifications. In brief, mice were anesthetized by intravenously injecting 2% phenobarbital sodium solution (20 mg/kg). Corneal surface anesthesia was performed by applying 0.4% (w/v) oxybuprocaine hydrochloride eye drop (Santen Pharmaceutical Co. Ltd, Japan) and a combination drop containing 0.5% phenylephrine and 0.5% tropicamide (Mydrin-P, Santen, Japan). The needle was inserted to the center of the vitreous under direct visualization. One microliter of 10 mg/mL conbercept solution was injected into the vitreous with HAMILTON needle of the correct eye and 1 μL of identical vehicle solution was injected into the left eye as a control. The needle was inserted behind the limbus through the pars plana at an oblique angle to avoid damaging the crystallized lens. To forestall the injected solution from escaping the attention once the needle was withdrawn, the needle tip was command within the eye for 30s once the injection.

Retina Isolation and Isolectin Staining of Retinal Vasculature To visualize retinal vasculature in fixed tissue, vessel staining and mouse retina preparation were performed as demonstrated by Tual-Chalot et al[29]. Postnatal mice were sacrificed by cervical dislocation and the surrounding tissues

and optic nerve were cut and the eyes were lifted up. Eyeballs were harvested and immersed in 4% paraformaldehyde (PFA) at room temperature. After fixing with PFA for 10-15min, uveal tissue, cornea, sclera and lens were removed from the retina. The isolated retina was stored in the phosphate buffered saline (PBS) and cut partially at four places along the rim to allow the tissue to be flattened on the microscope slides. Cold (-20℃) methanol was then added onto surface of retina to fix the retinas and facilitated permeabilization. Then retinas were incubated with the endothelial cell-specific marker and isolectin-B4 at 4℃ for overnight, and followed by 4,6-diamidino-2-phenylindole (DAPI) nucleic acid staining. Images were captured by immunofluorescence using a Nikon OFN25 microscope (4×).

Protein Purification The protein samples were from 8 mice retinas in each group, but Group 1 (Normal17) was not included. The retinal tissue was dropping into liquid nitrogen and grinding into the fine powder and then transferred to a 5-mL centrifuge tube. Adding four volumes of lysis buffer (8 mol/L urea, 1% protease inhibitor cocktail; Calbiochem, Merck, Germany) to the fine tissue powder, followed by sonication three times on ice using a high intensity ultrasonic processor (Ningbo Scientz Biotechnology Co., Ltd, China). The homogenate was then centrifuged at 12 000 g at 4℃ for 10min. The retinal protein extract was collected from the supernatant. The protein concentration of each retina was measured by the bicinchoninic acid (BCA) protein assay kit (Beyotime, Jiangsu Province, China).

Trypsin Digestion The retinal protein extraction was reacted with 5 mmol/L dithiothreitol (Sigma-Aldrich, USA) for 30min at 56℃ and alkylated with 11 mmol/L iodoacetamide (Sigma-Aldrich, USA) for 15min at room temperature in darkness. The treated protein sample was diluted by adding 100 mmol/L triethylammonium bicarbonate (TEAB, Sigma-Aldrich, USA) to urea (Sigma-Aldrich, USA) concentration less than 2 mol/L. At last, the first and second digestion were using trypsin-to-protein mass ratio at 1:50 (overnight), 1:100 (4h), respectively. (Trypsin, Promega corporation, USA).

TMT Labeling Trypsin digested peptides were desalted by Strata X C18 SPE column (Phenomenex, USA) and vacuum-dried. Peptide then was reconstituted in 0.5 mol/L TEAB and processed according to the tandem mass tag kit (TMT; Thermo Fisher Scientific, USA) protocol. One unit of TMT reagent was thawed and reconstituted in acetonitrile (Thermo Fisher Scientific, USA). The peptide mixtures were incubated for 2h at room temperature, and desalted, pooled and dried by the vacuum centrifugation.

HPLC Fractionation The tryptic peptides were then separated by high pH reverse-phase HPLC using Agilent 300 Extend C18 column (5 μm particles, 4.6 mm ID, 250 mm length, Agilent Technologies, USA). Peptides were separated into 60 fractions with a gradient of 8% to 32% acetonitrile (pH 9.0) for about 60min. Further, the peptides were separated into 18 fractions and dried by the vacuum centrifugation.

LC-MS/MS Analysis The tryptic peptides were dissolved in 0.1% acid (solvent A, Fluka, Sigma-Aldrich, USA), directly loaded onto a home-made reversed-phase analytical column (15-cm length, 75-μm inner diameter). The gradient was composed of a rise from 6% to 23% solvent B (0.1% formic acid in 98% acetonitrile) over 26min, 23% to 35% in 8min and climb to 80% in 3min then holding at 80% for 3min, all at a continuing rate of 400 nL/min on associate degree EASY-nLC 1000 UPLC system. The peptides were subjected to the nano-spray-ionization (NSI) supply followed by tandem mass spectrum analysis (MS/MS) in Q ExactiveTM Plus (Thermo Fisher Scientific, USA) coupled on-line to the UPLC. The electrospray voltage applied was a 2.0 kV. The m/z scan vary was 350 to 1800 for full scan, and intact peptides were detected within the Orbitrap at a resolution of 70 000. Peptides were then designated for MS/MS exploitation NCE setting as twenty eight and therefore the fragments were detected within the Orbitrap at a resolution of 17 500. A data-dependent procedure that alternated between one MS scan followed by twenty MS/MS scans with 15.0s dynamic exclusion.

Data Processing and Library Searching The MS/MS raw data were processed using Maxquant search engine (v.1.5.2.8). Tandem mass spectra were searched against mice database concatenated with reverse decoy database. Trypsin/P was specified as the cleavage enzyme allowing up to 2 missing cleavages. First search range was set to 5 ppm for precursor ions and main search range was set to 5 ppm and 0.02 Da for the fragment ions. Carbamidomethyl on Cys was specified as the fixed modification and oxidation on Met was specified as variable modifications. False discovery rates (FDR) were adjusted to <1% and minimum score for peptides was set >40.

Statistical and Bioinformatic Analysis The proteomics analysis was used to analyze the retinal proteomic alterations in which bioinformatic tools were applied to study their associated biological pathways and functions. Statistical significant was set at $P < 0.05$.

Functional Enrichment Analysis Pathway enrichment analyses were widely used to analyze high-throughput data and help link individual proteins, which were differentially expressed under experimental disease and treatment conditions, in order to improve understanding regarding biological pathways[30].

Gene Ontology The Gene ontology (GO) annotation proteome was derived from the UniProt-GOA database (http://www.ebi. ac.uk/GOA/). We converted identified protein ID to UniProt ID and mapped to GO IDs. The unidentified proteins were use the InterProScan soft to annotate protein's GO functional

based on aligning the protein sequence. Furthermore, GO annotated proteins were classified in three categories: cellular component, biological process and molecular function.

KEGG Pathway Analysis KEGG automatic annotation server (KAAS) was used to annotate the protein's KEGG database description and mapped the annotation result on the KEGG pathway database. The KEGG database identified enriched pathways by a two-tailed Fisher's exact test to test the enrichment of the differentially expressed protein against all identified proteins. Standard false discovery rate control methods were use to correct multiple hypothesis testing.

DAVID Analysis As a comprehensive set of functional annotation tools, the Database for Annotation, Visualization and Integrated Discovery (DAVID; https://david.ncifcrf. gov/) had been used for systematic and integrative analysis to characterize the function of the identified proteins in the quantitative proteomics analysis. Also, DAVID was applied to the functional enrichment studies in GO analyses and KEGG pathway, following the protocol in 2009[31].

Protein-Protein Interaction Network The protein-protein interaction (PPI) analysis used to explore the molecular mechanisms. In this study, we applied Search Tool for the Retrieval of Interacting Genes (STRING; http://string-db.org/) database to construct PPI network, and the protein interaction was applied to the protein interaction and GO analyses, following the protocol in 2015[32].

RESULTS

Effects of Conbercept on Retinal Neovascularization in OIR Mice Mice treated with conbercept were presented in Figure 1A. Neonatal mice were placed under hyperoxic conditions (75% O_2) for 5d to produce retinal vaso-obliteration. Next, the mice were returned to normoxia (room air) to induce ischemic retinal neovascularization and treated with conbercept for 5d. The Isolectin b4 binds to the sugar residues of the glycocalyx in the retina blood vessels. Mice with retinas treated room air (Normal17) had fewer small vessels compared to the retina vessels treated high oxygen (OIR12/EXP1). The oxygen damaged retina had loss the main vessel and center vessel node in non-treated OIR mice (OIR17/Control) compared to conbercept treated mice (Lang17/EXP2; Figure 1B). The reduction difference of the avascular area and the extent of neovascularization were evaluated by relating the area covered by avascular area to the total retinal area (Figure 1C) and by observing clusters and tufts of blood vessels. Branching point analysis of TRITC-lectin-stained retinae from Normal17, OIR12/EXP1, OIR17/Control, and Lang17/EXP2 mice showed a prematurely dense vessel network in OIR17/Control and Lang17/EXP2 in comparison to Normal17 mice, whereas the vessel density was reduced in OIR12/EXP1 mice (Figure 2).
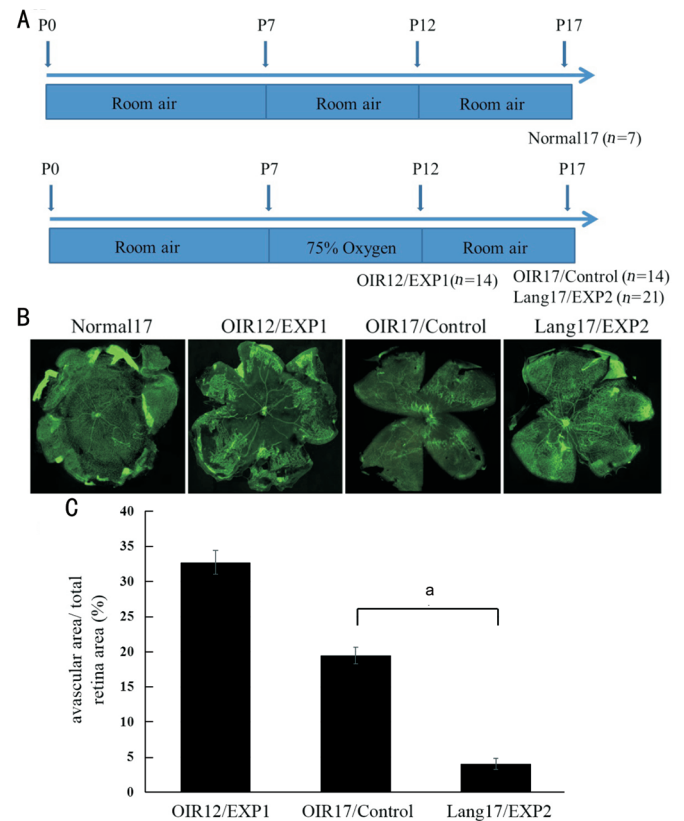

Figure 1 Effects of conbercept on retinal neovascularization at postnatal 17 in OIR mice A: Scheme of the OIR model and experimental designs. Group 1 (Normal17; n=7): mice were treated with normal air; Group 2 (OIR12/EXP1; n=14), mice received 75% oxygen from P7 to P12; group 3 (OIR17/Control; n=14), mice received 75% oxygen from P7 to P12 and then normal air to P17; and group 4 (Lang17/EXP2; n=21), mice received 75% oxygen from P7 to P12 with conbercept injection at P12, and then normal air from P12 to P17. B: The flat mounted retinas stained with Isolectin b4. C: The avascular area is given in % of the total retinal area. Results show means±SD; n=6/group; [a]P<0.05.

Disease and Repair Progression-associated Changes in Protein Expression on Retinas in OIR Mice LC-MS/MS analysis were performed to analyze the protein expression profiles of retina proteins in disease progression and repair in OIR mice with conbercept treatment. Three groups included OIR 12 (EXP1), OIR 17 (Control) and Lang17 (EXP2) were exanimated and used to evaluate the protein expression changes during three periods of disease (disease progression, repair-end, repair begin) in this study. The disease progression was investigated in the retina protein expression changes in 5d after oxygen treatment by comparing the protein expression of OIR 12 (EXP1) with OIR 17 (Control) group. Repair end were studied in the retina protein expression change in 5d after treatment by comparing the protein expression of Lang17 (EXP2) with OIR 17 (Control) group. Furthermore, by comparing the protein expression of OIR12 (EXP1) to Lang17 (EXP2) group, the protein changes induced by conbercept treatment (repair begin) were identified.
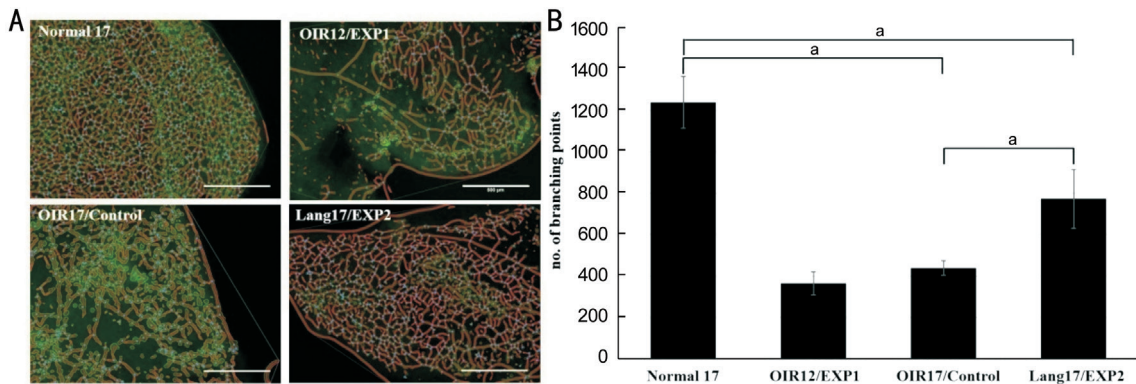
Figure 2 Conbercept influences retinal vascularization A: Fluorescence Isolectin b4 staining of the vascular structure of whole mount retina in Normal17, OIR12/EXP1, OIR17/Control and Lang17/EXP2 mice. Scale bar: 500 μm. B: Statistical analysis of the number of branching points in the retina of Normal17, OIR12/EXP1, OIR17/Control, and Lang17/EXP2 mice. Mean±SD, n=6, [a]P<0.05.
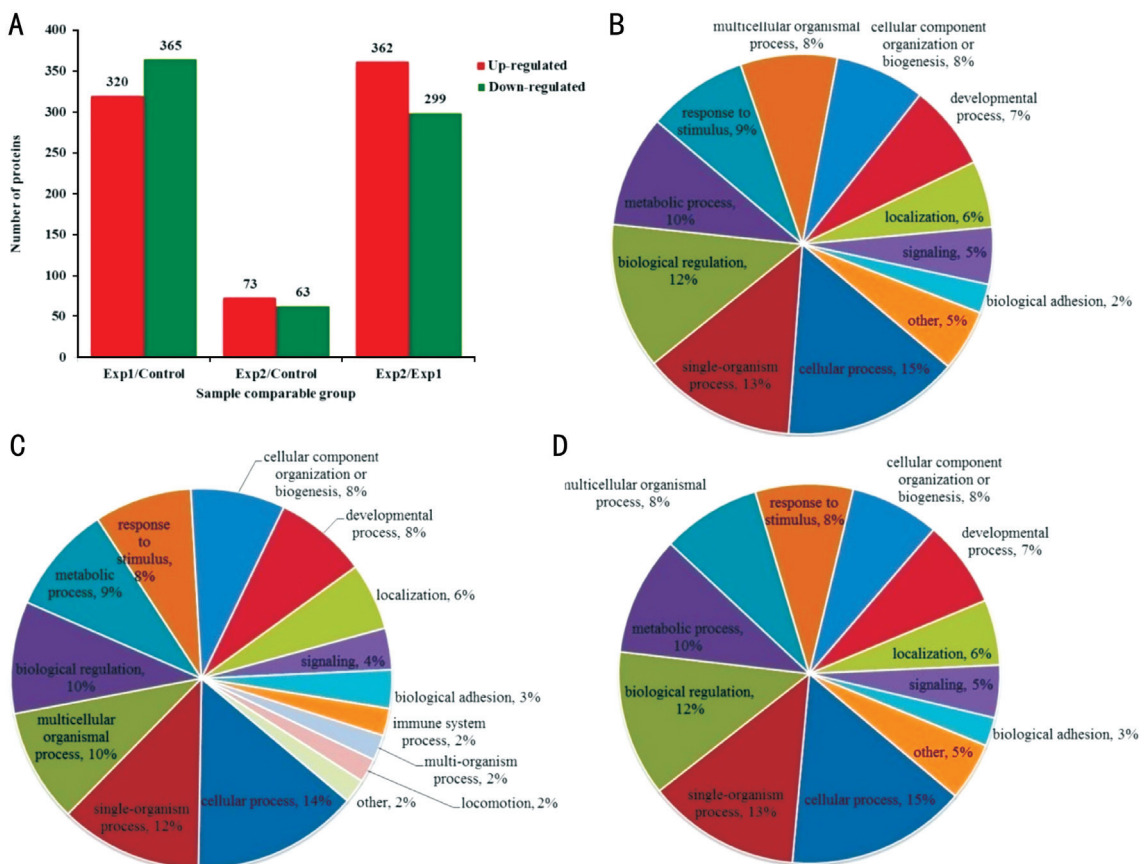
Figure 3 The GO analyses were performed to identify up- and down-regulated protein expression and associated functions in retinas during three periods: disease progression, repair end and repair begin A: Three periods were indicated at X-axis and numbers of protein were denoted at Y-axis. The up- and down-regulated protein were denoted in red and green, respectively. GO analysis classified the proteins into 3 groups (molecular function, biological process and cellular component). B: Disease period [OIR12 (EXP1)/Control]. C: Disease repair end [Lang17(EXP2)/Control]. D: Disease repair begin [EXP2 (Lang17)/EXP1 (OIR12)].

In the disease progression period, the expression ratio of 320 proteins were more than 1.3 and those of 365 protein expressions were down regulated (P<0.05). In the repair end period, 73 proteins were up-regulated, and 63 protein expressions were down-regulated (P<0.05). We found there was up-regulation of 362 proteins in the repair begin, and down-regulation of 299 proteins in the repair begin (Figure 3A, P<0.05).

GO Enrichment Analysis of Disease and Repair Progression-associated Proteins on Retinas in OIR Mice
We found that the proteins were changed in disease progression were involved in cellular process (15%), single-organism process (13%), biological regulation (12%) and metabolic process (10%) (Figure 3B). In the repair end, the proteins that were changed by conbercept treatment were involved in cellular process (14%), single-organism process (12%),

Figure 4 KEGG signaling pathways were analyzed with proteins during three periods including disease, repair end and repair begin The protein numbers were as indicated at X-axis and enriched pathways were denoted at Y-axis. A: Up-regulation proteins; B: Down-regulation proteins (enrichment score>2 and *P*<0.05).

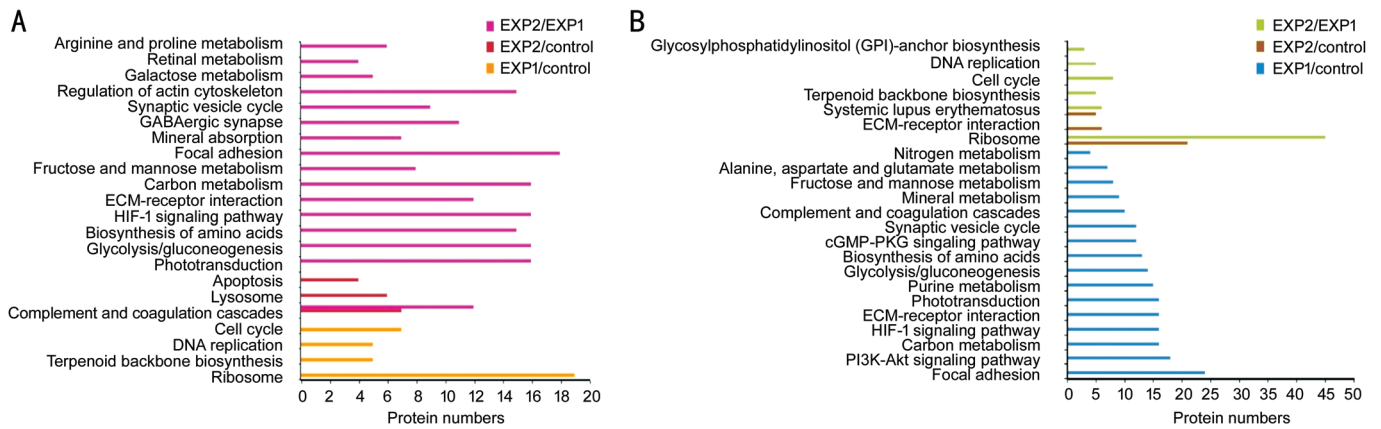multiple-organism process (10%) and biological regulation (10%) (Figure 3C). The conbercept treatment induced proteins changed in the repair begin period were involved in cellular process (15%), single-organism process (13%), biological regulation (12%) and metabolic process (10%) (Figure 3D). Although the main biological processes were practically the same among these three periods, the immune system (2%), locomotion (2%) and multiple-organism process (2%) were only presented in the repair end period. This result suggested that the different protein components were participated in the repair end compared with other two periods.

KEGG Signaling Pathways Analysis of Disease and Repair Progression-associated Proteins on Retinas in OIR Mice The numbers of up- and down-regulated proteins and their associated significantly enriched pathways during the disease and repair progression periods were presented at Figure 4A (up-regulation group) and 4B (down-regulation group). During both repair (begin and end), proteins associated in HIF-1, focal adhesion, photo-transduction, and complement and coagulation cascades pathways were up-regulated. However, proteins associated with these pathways during disease period were up-regulated in the OIR17 treatment group. The results showed that conbercept increased the regulation of proteins involved in HIF-1, focal adhesion, photo-transduction, and complement and coagulation cascades pathways yet inhibited proteins related to the cell cycle and DNA repair in the OIR17 treated groups. In addition, proteins involved in the extracellular matrix (ECM)-receptor interactions pathway were up-regulated in the repair begin period but down-regulated in the repair end. It was suggested that conbercept may initiated retinal fibrosis in OIR mice.

Up- and Down-regulated Proteins Induced by Conbercept after Oxygen-induced Retinopathy The numbers of proteins changed their expression in the disease and repair regression with expression ratio of disease progression, repair begin

and repair end periods more than 1.3 (*P*<0.05) were present in Figure 5A. We then further listed the up- and down-regulated proteins induced by the conbercept treatment in different combination period statuses in the OIR. We evaluated various regulation types in non-treated OIR mice (OIR17/Control) compared to conbercept treated mice (Lang17/EXP2) and achieved results as follows. Without change of protein expression in the disease progression period OIR, the effect of conbercept treatment on the proteins change had been investigated. In the repair progression, conbercept induced down-regulation of thirteen proteins and the up-regulation of thirteen proteins medicated by conbercept treatment in the OIR.

Along with the decreasing of protein expression in the disease progression period of OIR, effect of conbercept treatment on the proteins change had been explored. Two proteins were down-regulated in the repair end period and up-regulated in the repair begin period, including Zinc finger protein 428 (Znf428) and N-alpha-acetyltransferase 40 (Naa40). In addition, four proteins that were up-regulated in the repair end and unchanged in the repair begin include fatty acid-binding protein, epidermal (Fabp5), multiple epidermal growth factor-like domains protein 10 (Megf10), chloride intracellular channel protein 6 (Clic6) and protein tweety homolog 1 (ttyh1). Moreover, the conbercept treatment suppressed fourteen proteins in the repair progression.

With an increasing number of protein expression in the disease progression period of OIR, effect of conbercept treatment on the proteins change had also been studied. Six proteins were only down-regulated in the repair end not in the repair begin. In the repair begin, twenty proteins were increased and down-regulated in the repair begin. In addition, the conbercept treatment induced seventeen proteins increased expression during the disease progression period.

DAVID Analyses of Disease and Repair Progression-associated Proteins on Retinas in OIR Mice The potential

Figure 5 Functional enrichment analysis of gene ontology terms of the conbercept regulated proteins A: Summary of the combination status in up and down regulation types by expression ratio more than 1.3 (*P*<0.05). Results were summarized as number of protein (Y-axis). –, no change; ↑, up regulation type; ↓, down regulation type. B: GO-based annotation was based on the up-regulated proteins mediated by conbercept using the DAVID (v6.8) and String (v10.5) functional enrichment analysis tools. C: GO-based annotation was based on the down-regulated proteins mediated by conbercept using the DAVID (v6.8) and String (v10.5) functional enrichment analysis tools.

function of different protein expressions and their associated signally pathways in the repair end were shown in Figure 5B and 5C. Most of up-regulated proteins involved in eye development in the repair end (Figure 5B). During the repair end, the down-regulated proteins were related to translation and focal adhesion pathways and protein expression were increased in the ribonucleoprotein and intracellular proteins (Figure 5C). The results showed proteins that down-regulated in the repair end period were involved in metabolic process and angiogenesis. The proteins could increase complement and coagulation cascades, negative regulation of apoptotic process, blood coagulation, and fibrin clot formation.

PPI Network Construction The interaction score from experiments and databases was medium confident (0.400). The up-regulated proteins analyzed were included up-regulated proteins in repair end, such as fibroblast growth factors (FGF) 2 and Cryab. The two major networks included that ApoE, Fgg, Fga and F13a1 interacted with Clu, and Crygd, Crygs, Cryaa and Crybb1 interacted with Cryab (Figure 6A). The down-regulated proteins analyzed included down-regulated proteins in repair end period, such as Hspg2 and Uba52. The two major interaction networks included that the group of ribosomal proteins, H3F3A, H2AFX, Hist1h1d and Hist1h1a interact with Uba52. Another network is Lamc1, Lamb1, Col4a2 and Cspg4 interact with Hspg2 (Figure 6B).

DISCUSSION

Conbercept has demonstrated excellent efficacy with a long half-life and greater potential in dealing with VEGF-related retinal neovascularization[9]. To identify proteins for the treatment of OIR, we quantitatively analyzed the retinal proteome with conbercept treatment in mice with OIR. Through proteomic analysis of mice retinas, we tend to find that OIR molecular risk factors and fibrosis-related cytokines had been elicited by conbercept treatment, which can doubtless distress the physiological equilibrium towards the tube-shaped structure development in retinas. Our results from LC-MS/MS and isotope labeling-based relative quantification of macromole expression indicated that distinguished molecular activity in OIR mice with conbercept treatment were associated with OIR controls. Major molecular responses were detected within the OIR together with varied parts of tissue structure machinery and sensory responses for the upkeep of tissue equilibrium. However, no proteomic alterations related to associate in progress death method were detected in conbercept treated retinas. In addition, this study may provide a validation for recent experimental discoveries from the OIR mouse model. Bevacizumab exposure in human retinal pigment epithelial cells and glial cells has been shown to induce the epithelial-of-mesenchymal transition which may contribute to the possible formation of retinal fibrosis[33]. However, we found that conbercept treatment in OIR mice induced fibrosis-related cytokines and mechanisms mediated different pathways. We also observed that the FGF2 and HIF-1 signaling pathways were involved in the conbercept treatment. Therefore, more comprehensive studies in understanding of the fibrosis-related cytokines and mechanisms induced by conbercept were required. We had presented that proteins down-regulated in the repair end period, but up-regulation in the disease progression and repair begin period were involved in ECM pathways including ECM-receptor interaction, ECM organization, extracellular
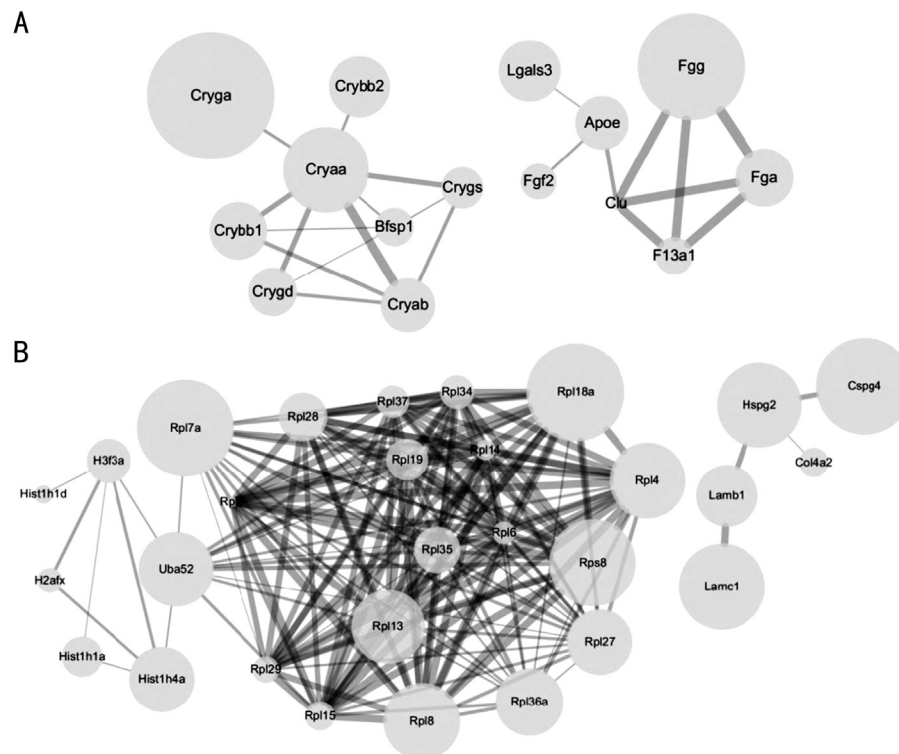
Figure 6 Protein-protein interaction network of proteins mediated by conbercept treatment in OIR Conbercept had increased the fibrosis factors expression and down-regulated the angiogenic proteins and angiogenic factors expression. A: The increased fibrosis proteins were associated with fibronectin pathways; B: The down-regulated angiogenic proteins were in the transcriptional activation. Node size was shown the fold change of EXP2/Control and edge thickness was indicated by the strength of data support.

exosome and glycoprotein. These proteins consist of laminins family (Lamb1 and Lamc1), heparan sulfate proteoglycan 2 (HSPG2) and type IV collagenalpha 2 (COL4A2). Fibrosis requires a normal functioning vascular network, and its success in restoring the damaged tissue depends on the remodeling of ECM[10]. Laminins are major proteins in the basal lamina and the protein network foundation for most cells and organs[34-35]. The HSPG2 can modulate the signaling of FGF 1, 2, and 18[36-37] and also bind to other heparin-binding growth factors including VEGF isoforms 165, 189 and 206, epidermal growth factor (EGF), transforming growth factor (TGF) α, connective tissue growth factor and hepatocyte growth factor (HGF). In addition, vascular smooth muscle cell proliferation occurs *via* FGF2 and plays a role for HSPG2 in the regulation of the FGF2 mediated proliferative responses[36]. HSPG2 is often thought as a pro-atherogenic molecule[38]. The vascular smooth muscle cell activation and proliferation is often inhibited by HSPG2[39]. Results from STRING analysis indicated that COL4A2 and chondroitin sulfate proteoglycan 4 (Cspg4) were interacted with VEGF-A, Flt (VEGF receptor-1) and KDR (VEGF receptor-2). Furthermore, COL4A2 was regulated by VEGF[40]. Our results showed that conbercept mediated down-regulated proteins consisting of Lamb1 and Lamc1, HSPG2 and COL4A2 were involved in ECM pathways, and associated with the fibrosis-related cytokines and mechanisms.

We also found the major proteins related to OIR including Cluserin (Clu), Fgg, Fga, and F13a1 were involved in the fibrosis. Clu deficiency was shown to be associated with renal inflammation and tissue fibrosis in the kidney through multiple pathways[41]. Fgg and Fga had also found to be involved in the fibrosis inranibizumab treatment[42]. Our study suggests potential target proteins including F13a1 were involved in retinal fibrosis, yet their associated molecular mechanisms required further investigations.

Proteins up-regulated in the three periods (with or without conbercept) were involved in complement and coagulation cascades (Fga and Fgg), negative regulation of apoptotic process (Cryab and Lgals3), and blood coagulation and fibrin clot formation (Fga and Fgg). Fga and Fgg were important renal pathology genes which involved in renal fibrosis[43]. ab-Crystallin (Cryab) had been reported as a key target for the development of drugs in the treatment of idiopathic pulmonary fibrosis (IPF) or other fibrotic diseases[44]. The key protein also increased the sub-retinal fibrotic lesions processes by modulating the epithelial-mesenchymal transition induced by transforming growth factor-β2 (TGFβ2)[45]. The TGFβ2 and FGF2 pathway also increased the vimentin expression to induced epithelial-mesenchymal transition[46]. In the study, vimentin reveal the relationship of FGF2 interaction network and Cryab interaction network. Galectin-3 (Lgals3) was shown

to be increased in a mouse model of bleomycin-induced lung fibrosis and in patients with IPF and interstitial pneumonia associated with collagen vascular disease (CVD-IP)[47].

The conbercept mediated fibrosis factors we found was fatty acid binding protein 5 (FABP5). The expression of FABP5 was down-regulated in the disease period yet upregulated in the repair end. FABP5 had 2.15-fold increase in human fibrotic skin tissues and regulated by the significant activation of the profibrotic TGF-β signaling pathway in human fibroblast[48]. However, this study was based on mouse retina, and the protein expression profile may be different from that in the human retinas. Nevertheless, this OIR mice model was consistent, reliable and suitable for studying the retina during the OIR.

In conclusion, in mice with OIR, we comprehensively examined the anti-angiogenic effects of conbercept *in vivo* and found that conbercept may effectively suppress ECM pathways. Conbercept appeared to induce specific fibrosis factors, which may serve as novel therapeutic targets to avoid fibrosis in the repeated conbercept injections. We suggested that the HIF-1 inhibitor combined with conbercept could be a promising strategy for the treatment of retinal angiogenic diseases.

REFERENCES

1 Kumar R, Mani AM, Singh NK, Rao GN. PKCθ-JunB axis via upregulation of VEGFR3 expression mediates hypoxia-induced pathological retinal neovascularization. *Cell Death Dis* 2020;11(5):325.

2 D'Amore PA. Mechanisms of retinal and choroidal neovascularization. *Invest Ophthalmol Vis Sci* 1994;35(12):3974-3979.

3 Casey R, Li WW. Factors controlling ocular angiogenesis. *Am J Ophthalmol* 1997;124(4):521-529.

4 Ishibazawa A, Nagaoka T, Yokota H, Takahashi A, Omae T, Song YS, Takahashi T, Yoshida A. Characteristics of retinal neovascularization in proliferative diabetic retinopathy imaged by optical coherence tomography angiography. *Invest Ophthalmol Vis Sci* 2016;57(14):6247-6255.

5 Rossino MG, Dal Monte M, Casini G. Relationships between neurodegeneration and vascular damage in diabetic retinopathy. *Front Neurosci* 2019;13:1172.

6 Michaelson IC. Vascular morphogenesis in the retina of the cat. *J Anat* 1948;82(Pt 3):167-174.4.

7 Ferrara N. Vascular endothelial growth factor. T*rends Cardiovasc Med* 1993;3(6):244-250.

8 McColm JR, Geisen P, Hartnett ME. VEGF isoforms and their expression after a single episode of hypoxia or repeated fluctuations between hyperoxia and hypoxia: relevance to clinical ROP. *Mol Vis* 2004;10:512-520.

9 Lu XM, Sun XD. Profile of conbercept in the treatment of neovascular age-related macular degeneration. *Drug Des Devel Ther* 2015;9:2311-2320.

10 Roy S, Amin S, Roy S. Retinal fibrosis in diabetic retinopathy. *Exp Eye Res* 2016;142:71-75.

11 Cornel S, Adriana ID, Mihaela TC, Speranta S, Algerino S, Mehdi B, Jalaladin HR. Anti-vascular endothelial growth factor indications in ocular disease. *Rom J Ophthalmol* 2015;59(4):235-242.

12 Yang XC, Xu JB, Wang RL, Mei Y, Lei H, Liu J, Zhang T, Zhao HY. A randomized controlled trial of conbercept pretreatment before vitrectomy in proliferative diabetic retinopathy. *J Ophthalmol* 2016;2016:2473234.

13 Nguyen TT, Guymer R. conbercept (KH-902) for the treatment of neovascular age-related macular degeneration. *Expert Rev Clin Pharmacol* 2015;8(5):541-548.

14 Amadio M, Govoni S, Pascale A. Targeting VEGF in eye neovascularization: What's new?: a comprehensive review on current therapies and oligonucleotide-based interventions under development. *Pharmacol Res* 2016;103:253-269.

15 Moreno TA, Kim SJ. Ranibizumab (lucentis) versus bevacizumab (avastin) for the treatment of age-related macular degeneration: an economic disparity of eye health. *Semin Ophthalmol* 2016;31(4):378-384.

16 Schaal S, Kaplan HJ, Tezel TH. Is there tachyphylaxis to intravitreal anti-vascular endothelial growth factor pharmacotherapy in age-related macular degeneration? *Ophthalmology* 2008;115(12):2199-2205.

17 Zhang Z, Yang X, Jin H, Qu Y, Zhang Y, Liu K, Xu X. Changes in retinal nerve fiber layer thickness after multiple injections of novel VEGF decoy receptor conbercept for various retinal diseases. *Sci Rep* 2016;6:38326.

18 Forooghian F, Cukras C, Meyerle CB, Chew EY, Wong WT. Tachyphylaxis after intravitreal bevacizumab for exudative age-related macular degeneration. *Retina* 2009;29(6):723-731.

19 Eghøj MS, Sørensen TL. Tachyphylaxis during treatment of exudative age-related macular degeneration with ranibizumab. *Br J Ophthalmol* 2012;96(1):21-23.

20 Li X, Xu G, Wang Y, Xu X, Liu X, Tang S, Zhang F, Zhang J, Tang L, Wu Q, Luo D, Ke X, AURORA Study Group. Safety and efficacy of conbercept in neovascular age-related macular degeneration: results from a 12-month randomized phase 2 study: AURORA study. *Ophthalmology* 2014;121(9):1740-1747.

21 Ethen CM, Reilly C, Feng X, Olsen TW, Ferrington DA. Age-related macular degeneration and retinal protein modification by 4-hydroxy-2-nonenal. *Invest Ophthalmol Vis Sci* 2007;48(8):3469-3479.

22 Sundstrom JM, Hernández C, Weber SR, Zhao Y, Dunklebarger M, Tiberti N, Laremore T, Simó-Servat O, Garcia-Ramirez M, Barber AJ, Gardner TW, Simó R. Proteomic analysis of early diabetic retinopathy reveals mediators of neurodegenerative brain diseases. *Invest Ophthalmol Vis Sci* 2018;59(6):2264-2274.

23 Wang JM, Lei CY, Tao LF, Wu Q, Ke X, Qiu YG, Lei B. A safety study of high concentration and high frequency intravitreal injection of conbercept in rabbits. *Sci Rep* 2017;7(1):592.

24 Kim SJ, Jin J, Kim YJ, Kim Y, Yu HG. Retinal proteome analysis in a mouse model of oxygen-induced retinopathy. *J Proteome Res* 2012;11(11):5186-5203.

25 Tu CJ, Beharry KD, Shen XM, Li J, Wang LS, Aranda JV, Qu J. Proteomic profiling of the retinas in a neonatal rat model of oxygen-induced retinopathy with a reproducible ion-current-based MS1 approach. *J Proteome Res* 2015;14(5):2109-2120.

26 Vadlapatla RK, Vadlapudi AD, Mitra AK. Hypoxia-inducible factor-1 (HIF-1): a potential target for intervention in ocular neovascular diseases. *Curr Drug Targets* 2013;14(8):919-935.

27 Smith LE, Wesolowski E, McLellan A, Kostyk SK, D'Amato R, Sullivan R, D'Amore PA. Oxygen-induced retinopathy in the mouse. *Invest Ophthalmol Vis Sci* 1994;35(1):101-111.

28 Chiu K, Chang RC, So KF. Intravitreous injection for establishing ocular diseases model. *J Vis Exp* 2007(8):313.

29 Tual-Chalot S, Allinson KR, Fruttiger M, Arthur HM. Whole mount immunofluorescent staining of the neonatal mouse retina to investigate angiogenesis *in vivo*. *J Vis Exp* 2013(77):e50546.

30 Mao XZ, Zhang Y, Xu Y. SEAS: a system for SEED-based pathway enrichment analysis. *PLoS One* 2011;6(7):e22556.

31 Huang DW, Sherman BT, Lempicki RA. Systematic and integrative analysis of large gene lists using DAVID bioinformatics resources. *Nat Protoc* 2009;4(1):44-57.

32 Szklarczyk D, Franceschini A, Wyder S, Forslund K, Heller D, Huerta-Cepas J, Simonovic M, Roth A, Santos A, Tsafou KP, Kuhn M, Bork P, Jensen LJ, von Mering C. STRING v10: protein-protein interaction networks, integrated over the tree of life. *Nucleic Acids Res* 2015;43(Database issue):D447-D452.

33 Zhang JJ, Chu SJ, Sun XL, Zhang T, Shi WY. Bevacizumab modulates retinal pigment epithelial-to-mesenchymal transition via regulating Notch signaling. *Int J Ophthalmol* 2015;8(2):245-249.

34 Simon T, Bromberg JS. Regulation of the immune system by laminins. *Trends Immunol* 2017;38(11):858-871.

35 Matlin KS, Myllymäki SM, Manninen A. Laminins in epithelial cell polarization: old questions in search of new answers. *Cold Spring Harb Perspect Biol* 2017;9(10):a027920.

36 Lord MS, Chuang CY, Melrose J, Davies MJ, Iozzo RV, Whitelock JM. The role of vascular-derived perlecan in modulating cell adhesion, proliferation and growth factor signaling. *Matrix Biol* 2014;35:112-122.

37 Knox S, Merry C, Stringer S, Melrose J, Whitelock J. Not all perlecans are created equal: interactions with fibroblast growth factor (FGF) 2

and FGF receptors. *J Biol Chem* 2002;277(17):14657-14665.

38 Tran-Lundmark K, Tran PK, Paulsson-Berne G, Fridén V, Soininen R, Tryggvason K, Wight TN, Kinsella MG, Borén J, Hedin U. Heparan sulfate in perlecan promotes mouse atherosclerosis: roles in lipid permeability, lipid retention, and smooth muscle cell proliferation. *Circ Res* 2008;103(1):43-52.

39 Kinsella MG, Tran PK, Weiser-Evans MC, Reidy M, Majack RA, Wight TN. Changes in perlecan expression during vascular injury: role in the inhibition of smooth muscle cell proliferation in the late lesion. *Arterioscler Thromb Vasc Biol* 2003;23(4):608-614.

40 Nillesen ST, Geutjes PJ, Wismans R, Schalkwijk J, Daamen WF, van Kuppevelt TH. Increased angiogenesis and blood vessel maturation in acellular collagen-heparin scaffolds containing both FGF2 and VEGF. *Biomaterials* 2007;28(6):1123-1131.

41 Guo J, Guan Q, Liu X, Wang H, Gleave ME, Nguan CY, Du C. Relationship of clusterin with renal inflammation and fibrosis after the recovery phase of ischemia-reperfusion injury. BMC Nephrol 2016;17(1):133.

42 Zou C, Han C, Zhao M, Yu J, Bai L, Yao Y, Gao S, Cao H, Zheng Z. Change of ranibizumab-induced human vitreous protein profile in patients with proliferative diabetic retinopathy based on proteomics analysis. *Clin Proteomics* 2018;15:12.

43 Schanstra JP, Bachvarova M, Neau E, Bascands JL, Bachvarov D. Gene expression profiling in the remnant kidney model of wild type and kinin B1 and B2 receptor knockout mice. *Kidney Int* 2007;72(4):442-454.

44 Bellaye PS, Wettstein G, Burgy O, Besnard V, Joannes A, Colas J, Causse S, Marchal-Somme J, Fabre A, Crestani B, Kolb M, Gauldie J, Camus P, Garrido C, Bonniaud P. The small heat-shock protein αB-crystallin is essential for the nuclear localization of Smad4: impact on pulmonary fibrosis. *J Pathol* 2014;232(4):458-472.

45 Ishikawa K, Sreekumar PG, Spee C, Nazari H, Zhu DH, Kannan R, Hinton DR. αB-crystallin regulates subretinal fibrosis by modulation of epithelial-mesenchymal transition. *Am J Pathol* 2016;186(4):859-873.

46 Kurimoto R, Ebata T, Iwasawa S, Ishiwata T, Tada Y, Tatsumi K, Takiguchi Y. Pirfenidone may revert the epithelial-to-mesenchymal transition in human lung adenocarcinoma. *Oncol Lett* 2017;14(1):944-950.

47 Nishi Y, Sano H, Kawashima T, Okada T, Kuroda T, Kikkawa K, Kawashima S, Tanabe M, Goto T, Matsuzawa Y, Matsumura R, Tomioka H, Liu FT, Shirai K. Role of galectin-3 in human pulmonary fibrosis. *Allergol Int* 2007;56(1):57-65.

48 Song J, Zhang H, Wang Z, Xu W, Zhong L, Cao J, Yang J, Tian Y, Yu D, Ji J, Cao J, Zhang S. The role of FABP5 in radiation-induced human skin fibrosis. *Radiat Res* 2018;189(2):177-186.